Inorganic Chemistry

Forum Article

pubs.acs.org/IC

In Pursuit of Homoleptic Actinide Alkyl Complexes

Lani A. Seaman,[†] Justin R. Walensky,*[,‡] Guang Wu,[†] and Trevor W. Hayton*[,†]

[†]Department of Chemistry and Biochemistry, University of California, Santa Barbara, California 93106, United States

[‡]Department of Chemistry, University of Missouri, Columbia, Missouri 65211, United States

Supporting Information

ABSTRACT: This Forum Article describes the pursuit of isolable homoleptic actinide alkyl complexes, starting with the pioneering work of Gilman during the Manhattan project. The initial reports in this area suggested that homoleptic uranium alkyls were too unstable to be isolated, but Wilkinson demonstrated that tractable uranium alkyls could be generated by purposeful "ate" complex formation, which serves to saturate the uranium coordination sphere and provide the complexes with greater kinetic stability. More recently, we reported the solid-state molecular structures of several homoleptic uranium alkyl complexes, including $[Li(THF)_4][U(CH_2{}^tBu)_5]$, $[Li(TMEDA)]_2[UMe_6]$, $[K(THF)]_3[K(THF)_2][U(CH_2Ph)_6]_2$, and $[Li(THF)_4][U(CH_2SiMe_3)_6]$, by employing Wilkinson's strategy. Herein, we describe our attempts to extend this chemistry to thorium. The treatment of $ThCl_4(DME)_2$ with 5 equiv of $LiCH_2{}^tBu$ or $LiCH_2SiMe_3$ at −25 °C in THF affords $[Th(CH_2{}^tBu)_5]$ (**1**) and $[Li(DME)_2][Th(CH_2SiMe_3)_5$ (**2**), respectively, in moderate yields. Similarly, the treatment of $ThCl_4(DME)_2$ with 6 equiv of $K(CH_2Ph)$ produces $[K(THF)]_2[Th(CH_2Ph)_6]$ (**3**), in good yield. Complexes **1**−**3** have been fully characterized, while the structures of **1** and **3** were confirmed by X-ray crystallography. Additionally, the electronic properties of **1** and **3** were explored by density functional theory.

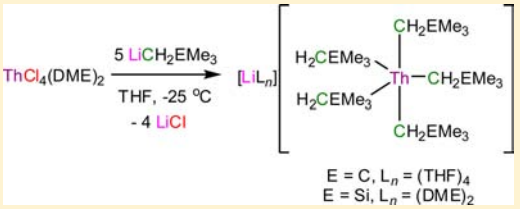

INTRODUCTION

History. The pursuit of isolable homoleptic uranium alkyl complexes has been ongoing since the 1940s.[1−8] This research was first motivated by the need for volatile uranium compounds for centrifugal isotope separation during the Manhattan project. Inspired by the volatility of main-group organometallics, such as $PbMe_4$,[2] Gilman and co-workers attempted the preparation of homoleptic uranium alkyls, including tetramethyluranium. Few experimental details were given in the original paper describing this work, but it was mentioned that the compounds were too unstable to be isolated.[1,2] Four decades later, the synthesis of homoleptic alkyls was revisited by Marks and Seyam.[3] They treated UCl_4 with 4 equiv of LiR (R = Me, $CH_2{}^tBu$, ^nBu, ^tBu, ^iPr) at low temperatures to generate "UR_4", which rapidly decomposed on warming.[3,7] The organic decomposition products were found to be mostly alkanes, and small amounts of alkenes, the latter likely formed by *β*-hydrogen elimination. For example, the reaction of UCl_4 with 4 equiv of *n*-BuLi in hexane reportedly yields 23.6% *n*-butane, 5.6% 1-butene, and 0.4% octane after 1 h at room temperature. They also concluded that U−C bond homolysis was not a major reaction pathway, based on the observation that the stereochemistry of the 2-*cis*-2-butenyl and 2-*trans*-2-butenyl fragments is retained upon thermolysis of the corresponding tetrakis(2-*cis*-2-butenyl)- and 2-*trans*-2-butenyluranium complexes.[9] Other groups have also explored the reactivity of UCl_4 with alkyllithium reagents and reported the formation of finely divided uranium metal.[3,5,9−11] However, Evans and co-workers thoroughly reinvestigated the reaction of UCl_4 with both *tert*-BuLi and *n*-BuLi and concluded that the likely product in these reactions was not uranium metal but a uranium(III) hydride, namely, UCl_2H.[6]

Recognizing that the coordinative unsaturation of the metal center in these complexes is a likely cause of their thermal instability,[4,12] Wilkinson and Sigurdson purposefully reacted UCl_4 with an excess of alkyllithium reagents to produce 'ate' complexes. These reactions afforded isolable, homoleptic alkyl 'ate' species with the formulation $[Li(solvent)_4]_2[UR_6]$ (solvent = THF, Et_2O; R = Me, C_6H_5, CH_2SiMe_3).[4] These molecules were characterized by ^1H NMR spectroscopy, magnetic susceptibility, and, where possible, elemental analysis. In addition, the reaction of excess LiR (R = Me, $CH_2{}^tBu$, CH_2SiMe_3) with $U_2(OEt)_{10}$ in dioxane was reported to provide the uranium(V) octa(alkyl) complexes $[Li(dioxane)]_3[UR_8]$. However, the formulation of both the uranium(IV) and -(V) complexes, in the absence of solid-state structural data, was later called into question.[12]

In parallel with the efforts of Wilkinson, Thiele and co-workers reported the synthesis of $U(CH_2Ph)_4{\cdot}MgCl_2$. Separation of $MgCl_2$ from the uranium component could not be achieved. Additionally, the compound reportedly decomposed above 130 °C.[13] Other than elemental analysis, little characterization of this material was provided, but it is likely that the ability of the benzyl ligand to adopt multidentate coordination modes provides enhanced kinetic stability. Similarly, Andersen and co-workers discovered that "UR_4"-type complexes could be

Special Issue: Inorganic Chemistry Related to Nuclear Energy

Received: April 27, 2012
Published: June 20, 2012

   dx.doi.org/10.1021/ic300867m | *Inorg. Chem.* 2013, 52, 3556−3564

stabilized by the addition of phosphines,[14] which allowed them to isolate the well-characterized complexes $AnR_4(dmpe)_n$ (An = U, Th; R = Me, CH_2Ph; n = 1, 2).[14,15] Finally, in 1989 Sattelberger and co-workers synthesized the first well-characterized homoleptic actinide alkyl, namely, $U[CH(SiMe_3)_2]_3$, by the reaction of $U(O\text{-}2,6\text{-}{}^tBu_2C_6H_3)_3$ with 3 equiv of $LiCH(SiMe_3)_2$.[8] While not coordinatively saturated, kinetic stabilization of this complex is afforded by the extremely bulky $-CH(SiMe_3)_2$ ligand. In the solid state, $U[CH(SiMe_3)_2]_3$ exhibits a trigonal-pyramidal geometry, similar to that of $U(N(SiMe_3)_2)_3$,[16] which has piqued the interest of theoreticians.[17,18]

In 2009, our research group reinvestigated the syntheses reported by Wilkinson and Sigurdson. We found that the reaction of UCl_4 with 5 equiv of LiR (R = $CH_2{}^tBu$, CH_2SiMe_3) produced $[Li(solvent)_x][UR_5]$ (solvent = DME, THF) in good yields (Scheme 1).[19] Both complexes were fully characterized,

Scheme 1

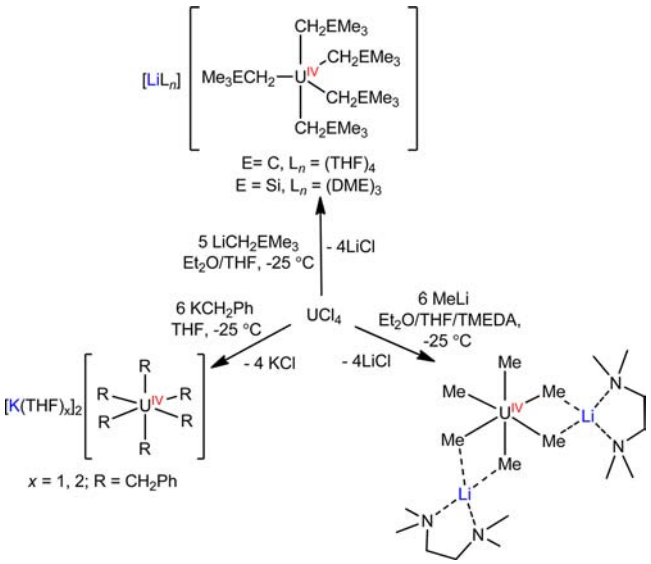

including analysis by X-ray crystallography in the case of R = $CH_2{}^tBu$. This complex exhibits a trigonal-bipyramidal structure about uranium. The (trimethylsilyl)methyl analogue was presumed to be isostructural, based on the structural characterization of trigonal-bipyramidal $[Li_{14}(O^tBu)_{12}Cl][U(CH_2SiMe_3)_5]$.[19] Interestingly, no evidence for the formation of octahedral $[UR_6]^{2-}$-type complexes was observed, even when 6 equiv of LiR were used in the reaction. Thus, it seems likely that Wilkinson and Sigurdson originally isolated $[Li(solvent)_x][UR_5]$-type complexes, instead of the proposed hexa(alkyl) species.

We also prepared a homoleptic uranium(IV) methyl complex, $[Li(TMEDA)]_2[UMe_6]$, by the reaction of UCl_4 with 6 equiv of MeLi, in the presence of excess TMEDA (Scheme 1). In the solid state, this complex exhibits an octahedral geometry about the uranium center, unlike its transition-metal counterparts (vide infra), which display trigonal-prismatic geometries, suggesting that there is little involvement of the 6d orbitals in the U−C σ bond.[19] This complex is quite temperature-sensitive and decomposes rapidly above −25 °C, both in solution and in the solid state. Additionally, the reaction of UCl_4 with 6 equiv of $K(CH_2Ph)$ in THF results in the formation of $[K(THF)]_3[K(THF)_2][U(CH_2Ph)_6]_2$ as a deep-red solid in good yield (Scheme 1). In the solid state, this complex exists as an extended 3D solid, in which $[U(CH_2Ph)_6]^{2-}$ monomers are linked via arene···K^+ bridging interactions. Notably, all of the benzyl groups exhibit an η^1-coordination mode.

$[Li(DME)_3][U(CH_2SiMe_3)_5]$ has proven to be amenable to further synthetic elaboration. For example, the reaction of $[Li(DME)_3][U(CH_2SiMe_3)_5]$ with 0.5 equiv of I_2, followed by 1 equiv of $Li(CH_2SiMe_3)$, in Et_2O at −25 °C, leads to the formation of a novel homoleptic uranium(V) alkyl, $[Li(THF)_4][U(CH_2SiMe_3)_6]$.[20] In the solid state, $[Li(THF)_4][U(CH_2SiMe_3)_6]$ exhibits an octahedral geometry. Further oxidation of this complex to uranium(VI) is also possible. Thus, the treatment of $[Li(THF)_4][U(CH_2SiMe_3)_6]$ with $U(O^tBu)_6$ in THF (Scheme 2) cleanly generates $U(CH_2SiMe_3)_6$, according to ^1H NMR spectroscopy. The solid-state molecular structure of $U(CH_2SiMe_3)_6$ would be of significant interest; however, this material is quite thermally sensitive and rapidly decomposes above −25 °C, making its isolation an experimental challenge.

More recently, Bart and co-workers reported the synthesis of base-free $U(CH_2Ph)_4$, by alkylation of UCl_4 with $K(CH_2Ph)$ in THF.[21] In the solid state, this complex features a pseudotetrahedral arrangement of four η^4-benzyl ligands. This complex is thermally sensitive, generating toluene and bibenzyl upon standing. Also of note, the addition of the redox-active $^{Mes}DAB^{Me}$ ligand [$^{Mes}DAB^{Me}$ = ArN=C(Me)C(Me)=NAr; Ar = 2,4,6-$Me_3C_6H_2$] to $U(CH_2Ph)_4$ results in the formation of $(^{Mes}DAB^{Me})U(CH_2Ph)_2$ and 1 equiv of bibenzyl, via a reductive elimination pathway.[21] In related work, Diaconescu and co-workers reported the in situ formation of "$U(CH_2Ph)_3(THF)_n$", which they subsequently used to prepare a pyridinyldi(amido) complex.[22]

In contrast to the rich chemistry reported for uranium, there has been limited progress toward the synthesis and characterization of homoleptic thorium alkyl complexes. To date, only one homoleptic thorium alkyl complex has been structurally characterized, namely, the heptamethyl complex $[Li(TMEDA)]_3[ThMe_7]$.[23] The complex exhibits a distorted monocapped trigonal-prismatic geometry, which differs from the six-coordinate geometry found for $[Li(TMEDA)]_2[UMe_6]$.[19] This difference is likely due to the larger ionic radius of Th^{IV} versus U^{IV} (for CN = 6: U^{4+} = 89

Scheme 2

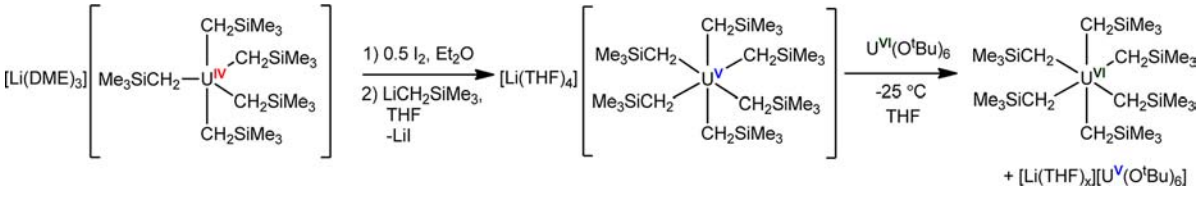

dx.doi.org/10.1021/ic300867m | Inorg. Chem. 2013, 52, 3556−3564

Scheme 3

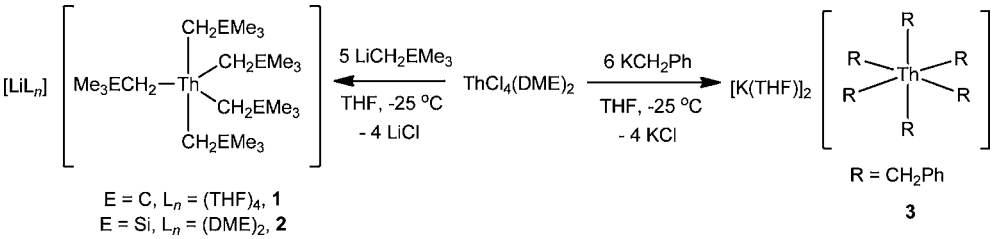

pm, Th^{4+} = 94 pm).[24] The homoleptic benzyl complexes $Th(CH_2\text{-}3,5\text{-}Me_2C_6H_3)_4$[25] and $Th(CH_2Ph)_4$[26] have also been reported, but their structures have not been confirmed by X-ray crystallography, although a phosphine adduct of $Th(CH_2Ph)_4$, namely, $Th(CH_2Ph)_4(dmpe)$, has been structurally characterized.[14] Finally, $Th(CH_2SiMe_3)_4(DME)_n$ was prepared by the reaction of $ThCl_4(DME)_2$ and 4 equiv of $LiCH_2SiMe_3$, but its isolation was hampered by its thermal instability.[27]

Structure and Bonding. Interest in high-valent, homoleptic organometallic complexes has not been restricted to the actinides. In fact, transition metal complexes of the type $[MR_6]^n$ (R = alkyl, aryl, H; n = 0, −1, −2) have been the focus of intense theoretical and experimental scrutiny.[28−42] Interest in this area was spurred by the observation that $[Li(TMEDA)]_2[ZrMe_6]$ exhibits a trigonal-prismatic D_{3h} geometry in the solid state.[38] Similarly, an X-ray crystallographic determination of WMe_6 by Seppelt and Pfennig revealed a distorted trigonal-prismatic C_{3v} geometry,[35,43,44] confirming the results of an earlier gas-phase electron diffraction study.[45] Since these pioneering studies, many homoleptic complexes exhibiting trigonal-prismatic structures have been structurally characterized, including $ReMe_6$, $[Ta(C{\equiv}CSi^tBu_3)_6]^-$, $[M(C_6H_5)_6]^-$ (M = Nb, Ta), and $[Zr(SC_6H_4\text{-}p\text{-}Me)_6]^{2-}$.[35,36,46−49]

Many theoretical studies have been performed to uncover the electronic structures responsible for this geometry preference. Interestingly, both molecular orbital and valence-bond analyses predict an energetic preference for trigonal-prismatic geometries in systems where $d^n \leq 1$ and the metal is ligated by σ-only ligands.[28−30,32−34,39−41,50] In these systems, the distortion away from O_h is favored because it allows for greater metal d-orbital involvement in the metal−ligand bond,[28−30,32,34,35,37,51,52] resulting in a strengthening of the σ interaction.[29,30] Electronic configurations with $d^n > 1$ force the p orbitals to participate in M−R bonding, thereby favoring an octahedral geometry.[29,30,35,37] Thus, the observation of a nonoctahedral geometry is evidence for d-orbital involvement in metal−ligand bonding. This final point is of particular importance to actinide chemists, who are currently engaged in an intense effort to quantify the participation of the 6d and 5f orbitals in An−L bonding.[53−67] However, all three structurally characterized $[UR_6]^n$-type complexes (n = −1, −2; R = Me, CH_2Ph, CH_2SiMe_3) isolated thus far exhibit octahedral geometries.[19,20] This difference in the geometry preference can be explained by the ability of uranium to engage its f orbitals in bonding. The *ungerade* character of the 5f orbitals, like the *ungerade* character of the p orbitals, should enforce an octahedral geometry for six-coordinate complexes.[37,65,68,69] In fact, f-orbital participation in $[U(CH_2SiMe_3)_6]^-$ is predicted to be significant. For example, the HOMO−1, HOMO−2, and HOMO−3 orbitals (HOMO = highest occupied molecular orbital) in $[U(CH_2SiMe_3)_6]^-$, which comprise the t_{1u} set, exhibit ca. 29% 5f-orbital participation.[20] Alternately, an octahedral geometry is also expected if M−L bonding is predominantly ionic,[70] a fact that likely explains the octahedral geometries observed for $[Li(TMEDA)]_3[LnMe_6]$ (Ln = Ho, Er, Lu).[71−73] The synthesis and characterization of new homoleptic actinide alkyl complexes could help untangle these effects, and in this context, thorium is especially interesting because its f orbitals are thought to be too high in energy to interact with the ligands, leaving the d orbitals as the primary orbitals for forming M−L bonds.[57,74] These observations prompted us to explore the synthesis of new homoleptic thorium alkyl complexes.

RESULTS AND DISCUSSION

Synthesis. We initially attempted to prepare a homoleptic six-coordinate $[ThMe_6]^{2-}$ complex, for comparison with the uranium analogue, $[UMe_6]^{2-}$. However, the reaction of $ThCl_4(DME)_2$ with 6 equiv of MeLi in Et_2O at −25 °C, in the presence of TMEDA, results in the formation of the previously characterized $[Li(TMEDA)]_3[ThMe_7]$, as the only identifiable species by ^1H NMR spectroscopy (see the Supporting Information).[23] Its presence is marked by a singlet at 0.18 ppm in C_6D_6, assignable to the Th−CH_3 groups. This is identical with the chemical shift reported by Marks et al.[23] We also attempted to access $[ThMe_6]^{2-}$ by demethylation of $[Li(TMEDA)]_3[ThMe_7]$.[23] Thus, the addition of 1 equiv of Me_3SiCl to $[Li(TMEDA)]_3[ThMe_7]$ in C_6D_6 results in the formation of a yellow solution and generation of a white precipitate (see the Supporting Information). The ^1H NMR spectrum reveals a sharp singlet at 0 ppm, assignable to $SiMe_4$. Also present is a broad resonance at 0.20 ppm, which we have assigned to the methyl protons of the starting material, $[Li(TMEDA)]_3[ThMe_7]$ (eq 1). No other methyl environments are observed. Performing the reaction on a preparatory scale leads only to isolation of the starting material in 45% yield. Attempts to abstract a methyl group with 1 equiv of NEt_3HCl produce similar results (see the Supporting Information). Thus, it appears that demethylation simply results in the re-formation of $[Li(TMEDA)]_3[ThMe_7]$ via methyl scrambling, with concomitant formation of an unobserved decomposition product.

$$[Li(TMEDA)]_3[ThMe_7] \xrightarrow[-LiCl,\ C_6D_6]{Me_3SiCl} [Li(TMEDA)]_3[ThMe_7] + Me_4Si + \text{decomposition} \quad (1)$$

Because of the presumed instability of $[ThMe_6]^{2-}$, we turned our attention to alkylating reagents with bulkier R substituents, namely, $LiCH_2{}^tBu$, $LiCH_2SiMe_3$, and KCH_2Ph. The addition of 5 equiv of $LiCH_2{}^tBu$ to a THF solution of $ThCl_4(DME)_2$ at −25 °C gives a pale-yellow solution. After recrystallization from

dx.doi.org/10.1021/ic300867m | Inorg. Chem. 2013, 52, 3556−3564

Et_2O, the five-coordinate neopentylthorium complex, $[Li(THF)_4][Th(CH_2{}^tBu)_5]$ (**1**), can be isolated in 50% yield as colorless crystals (Scheme 3). Similarly, the addition of 5 equiv of $LiCH_2SiMe_3$ to a THF solution of $ThCl_4(DME)_2$ at −25 °C produces a colorless solution. Crystallization from Et_2O/DME, provides $[Li(DME)_2][Th(CH_2SiMe_3)_5]$ (**2**) as a white solid in 54% yield. Notably, the addition of 6 equiv of either $LiCH_2{}^tBu$ or $LiCH_2SiMe_3$ to $ThCl_4(DME)_2$ also results in the formation of the five-coordinate complexes.

Complexes **1** and **2** are thermally unstable solid that can be stored indefinitely at −25 °C under an inert atmosphere. Both **1** and **2** are insoluble in hexane but are very soluble in Et_2O and THF. The ^1H NMR spectrum of **1** in THF-d_8 reveals resonances at +1.02 and −0.07 ppm, corresponding to the methyl and methylene protons, respectively. The $^{13}C\{^1H\}$ NMR spectrum in THF-d_8 features resonances at 117.96 and 37.58 ppm, assignable to the methylene and methyl carbons, respectively. A resonance at 39.14 ppm is assignable to the quaternary carbon. Finally, there is a single resonance at 0.50 ppm in the ^7Li NMR spectrum. The ^1H NMR spectrum of **2** in THF-d_8 exhibits resonances at −0.01 and −0.63 ppm, corresponding to the methyl and methylene protons of the (trimethylsilyl)methyl ligand, respectively. Likewise, the $^{13}C\{^1H\}$ NMR spectrum in THF-d_8 exhibits resonances at 82.97 and 5.08 ppm, assignable to the methylene and methyl carbons of the (trimethylsilyl)methyl ligand, respectively. Finally, the ^7Li NMR spectrum in THF-d_8 exhibits a single resonance at −0.53 ppm.

Both **1** and **2** are stable in THF at room temperature for several hours, according to ^1H NMR spectroscopy, but after 24 h, evidence of decomposition is present in both samples. Both **1** and **2** are unstable in aromatic solvents. Dissolution of **1** in C_6D_6 results in immediate decomposition, affording a colorless solution in which neopentane is the only identifiable product, according to ^1H NMR spectroscopy. Complex **2** also decomposes immediately in the presence of C_6D_6, affording several unidentifiable resonances in the ^1H NMR spectrum. Similar results are observed in pyridine-d_5.

Complex **1** crystallizes in the monoclinic space group $P2_12_12_1$ with two crystallographically independent molecules in the asymmetric unit. They exhibit similar metrical parameters, and only one will be discussed in detail. In the solid state, **1** exhibits a trigonal-bipyramidal geometry about the thorium center (Figure 1) and is isostructural with its uranium(IV) analogue, $[Li(THF)_4][U(CH_2{}^tBu)_5]$.[19] The Th−C bond lengths range from 2.46(2) to 2.56(2) Å and are similar to those reported for $[Li(TMEDA)]_3[ThMe_7]$ [2.571(9)−2.723(8) Å] and other neosilyl and neopentyl thorium complexes [2.438(16)−2.54(2) Å].[23,27,75−77] Additionally, the Th−C−C bond angles range from 125(2)° to 148(2)°. These comparatively large angles may be evidence for α-agostic C−H−Th interactions. Emslie and co-workers observed similar angles in $[LTh(CH_2SiMe_3)_2]$ [L = 4,5-bis(2,6-diisopropylanilido)-2,7-di-*tert*-butyl-9,9-dimethylxanthene], which they determined were due to the presence of α-agostic C−H−Th interactions.[27]

We have also explored the reactivity of $ThCl_4(DME)_2$ with $K(CH_2Ph)$. The addition of 6 equiv of $K(CH_2Ph)$ to a THF solution of $ThCl_4(DME)_2$ at −25 °C results in the formation of a red-orange solution. Crystallization of this material from THF/hexane provides $[K(THF)]_2[Th(CH_2Ph)_6]$ (**3**) as a yellow-orange solid, in 80% yield (Scheme 3).

Complex **3** is a thermally unstable solid; however, it can be stored indefinitely at −25 °C under an inert atmosphere. It is insoluble in hexane and toluene but very soluble in THF. Its ^1H NMR spectrum in THF-d_8 exhibits resonances at 6.69, 6.27, 6.11, and 1.34 ppm, corresponding to the three aryl CH environments and the methylene protons, respectively. The $^{13}C\{^1H\}$ NMR spectrum in THF-d_8 at 0 °C exhibits very broad resonances at 153.0, 124.1, and 115.9 ppm, assignable to the carbon environments of the aryl ring. Additionally, a broad resonance at 89.6 ppm is assignable to the methylene resonance. We suggest that the broadness of the ^{13}C resonances is due to the fluxional behavior of the benzyl ligand (vide infra). Attempts to probe this behavior with variable-temperature $^{13}C\{^1H\}$ NMR spectroscopy were thwarted by the insolubility of **3** in cold THF, which prevents low-temperature spectra from being recorded, and its thermal sensitivity, which prevents high-temperature spectra from being recorded. For example, toluene is observed in a THF-d_8 solution of **3** after only 5 min at room temperature. Upon further standing, the solution turns orange-red and the resonances associated with **3** disappear, while those of toluene increase in intensity.

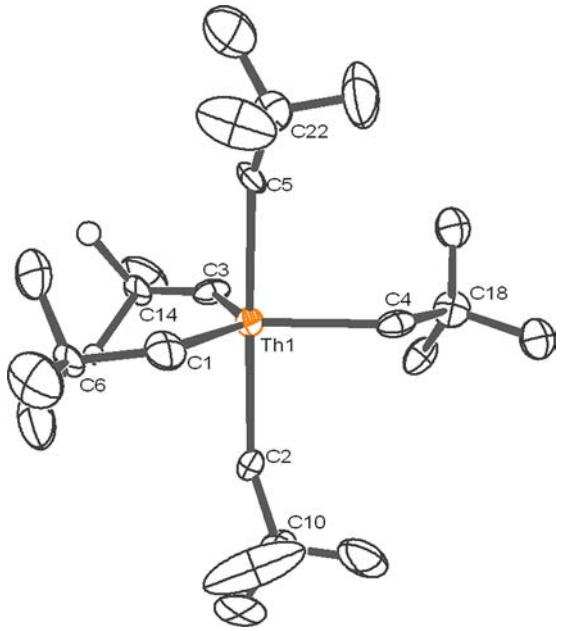

Figure 1. Solid-state molecular structure of **1** with 30% probability ellipsoids. $[Li(THF)_4]^+$ cation and hydrogen atoms excluded for clarity. Selected bond lengths (Å) and angles (deg): Th1−C1 = 2.52(3), Th1−C2 = 2.50(2), Th1−C3 = 2.56(2), Th1−C4 = 2.46(2), Th1−C5 = 2.53(2); Th1−C1−C6 = 131(2), Th1−C2−C10 = 145(2), Th1−C3−C14 = 129(2), Th1−C4−C18 = 125(2), Th1−C5−C22 = 148(2), C1−Th1−C3 = 132(1), C1−Th1−C4 = 116.4(9), C3−Th1−C4 = 111.4(8), C2−Th1−C5 = 173.0(9).

Complex **3** crystallizes in the monoclinic space group *Pn* and consists of two crystallographically independent thorium centers (Figure 2). Each thorium is coordinated by six benzyl ligands in a severely distorted octahedral geometry [e.g., C1−Th1−C5 = 73.4(6)°, C1−Th1−C4 = 114.6(5)°, C8−Th2−C9 = 115.5(6)°, and C7−Th2−C10 = 80.2(6)°]. This distortion is due to the presence of a multidentate benzyl ligand in each thorium coordination sphere.[14,78,79] For Th1, the multidentate benzyl ligand exhibits a Th−C(ipso) distance of Th1−C16 = 3.04(2) Å, while the corresponding Th−C_{benzyl} distance is Th1−C4 = 2.63(2) Å. Additionally, the Th−C−C angle is Th1−C4−C16 = 93(1)°, while the Th−C(ortho) distances are 3.28(2) and 3.91(2) Å. Overall, these metrical parameters are

dx.doi.org/10.1021/ic300867m | *Inorg. Chem.* 2013, 52, 3556−3564

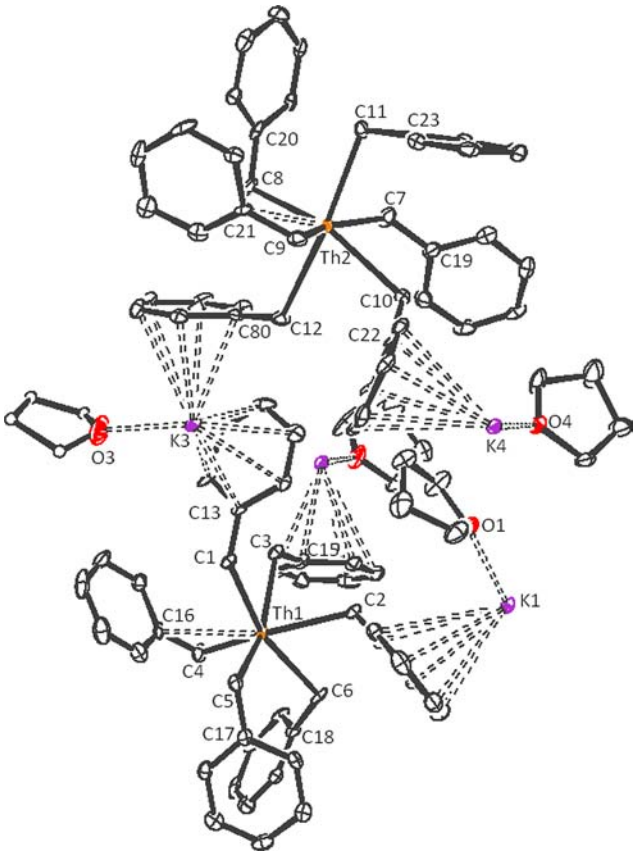

Figure 2. Solid-state molecular structure of **3** with 50% probability ellipsoids. Hydrogen atoms omitted for clarity. Selected bond lengths (Å) and angles (deg): Th1−C1 = 2.69(2), Th1−C2 = 2.62(2), Th1−C3 = 2.59(2), Th1−C4 = 2.62(2), Th1−C5 = 2.64(2), Th1−C6 = 2.66(1), Th2−C7 = 2.61(2), Th2−C8 = 2.67(2), Th2−C9 = 2.60(2), Th2−C10 = 2.63(2), Th2−C11 = 2.61(2), Th2−C12 = 2.69(2); Th1−C1−C13 = 124(1), Th1−C2−C14 = 121(1), Th1−C3−C15 = 113(1), Th−C4−C16 = 93(1), Th1−C5−C17 = 108(1), Th1−C6−C18 = 117(1), Th2−C7−C19 = 132(1), Th2−C8−C20 = 104(1), Th2−C9−C21 = 100(1), Th2−C10−C22 = 119(1), Th2−C11−C23 = 110(1), Th2−C12−C80 = 119(1).

consistent with the presence of an η^3-benzyl ligand within the coordination sphere of Th1.[14] For Th2, the multidentate benzyl ligand exhibits a Th−C(ipso) distance of Th2−C21 = 3.20(1) Å, while the corresponding Th−C_{benzyl} distance is Th2−C9 = 2.61(1) Å. The Th−C−C angle is Th2−C9−C21 = 100(1)°, while both Th−C(ortho) distances are >3.5 Å. These metrical parameters are consistent with the presence of an η^2-benzyl ligand within the coordination sphere of Th2.[14] The remaining benzyl ligands for both Th1 and Th2 exhibit metrical parameters consistent with η^1 coordination.[14] The Th−C_{benzyl} bond lengths for these ligands range from 2.59(2) to 2.69(2) Å and are comparable to the Th−C_{benzyl} bond lengths observed in the multidentate ligands and those seen in other actinide benzyl complexes.[14,80−83] For example, The U−C_{benzyl} distances in $[K(THF)]_3[K(THF)_2][U(CH_2Ph)_6]_2$ range from 2.50(2) to 2.57(2) Å.[19] In addition, there are four potassium cations in the asymmetric unit of **3**. Each potassium participates in three η^6-coordinated π interactions with three aryl rings,[84] resulting in the formation of an extended 3D solid. Similar π interactions have been observed in other systems,[84−86] including the uranium(IV) benzyl analogue $[K(THF)]_3[K(THF)_2][U(CH_2Ph)_6]_2$.[19] Unlike complex **3**, however, the uranium analogue exhibits no η^2-benzyl interactions, an observation that can be rationalized by the smaller ionic radius of U^{4+} versus Th^{4+}.

Theoretical Studies. Despite our inability to isolate $[ThMe_6]^{2-}$, we were interested in exploring its electronic structure by density functional theory (DFT), specifically to address its ground-state geometry. Calculations were performed at the B3LYP level on $[ThMe_6]^{2-}$ and allowed to optimize to the lowest-energy geometry. A single-point calculation was also performed using an idealized octahedral geometry. Interestingly, the fully optimized structure for $[ThMe_6]^{2-}$ exhibits D_{3h} symmetry and is estimated to be 78.6 kcal/mol lower in energy than the octahedral case.[28,65] The C−Th−C bond angles are 76.9, 86.4, and 121.4°, while the Th−C bond distances are ca. 2.66 Å. In D_{3h} symmetry (Figure 3), the HOMO, which has A_2'' symmetry, exhibits 3% f character. HOMO−1 and HOMO−2 (E′) are doubly degenerate and contain 8% 6d character.

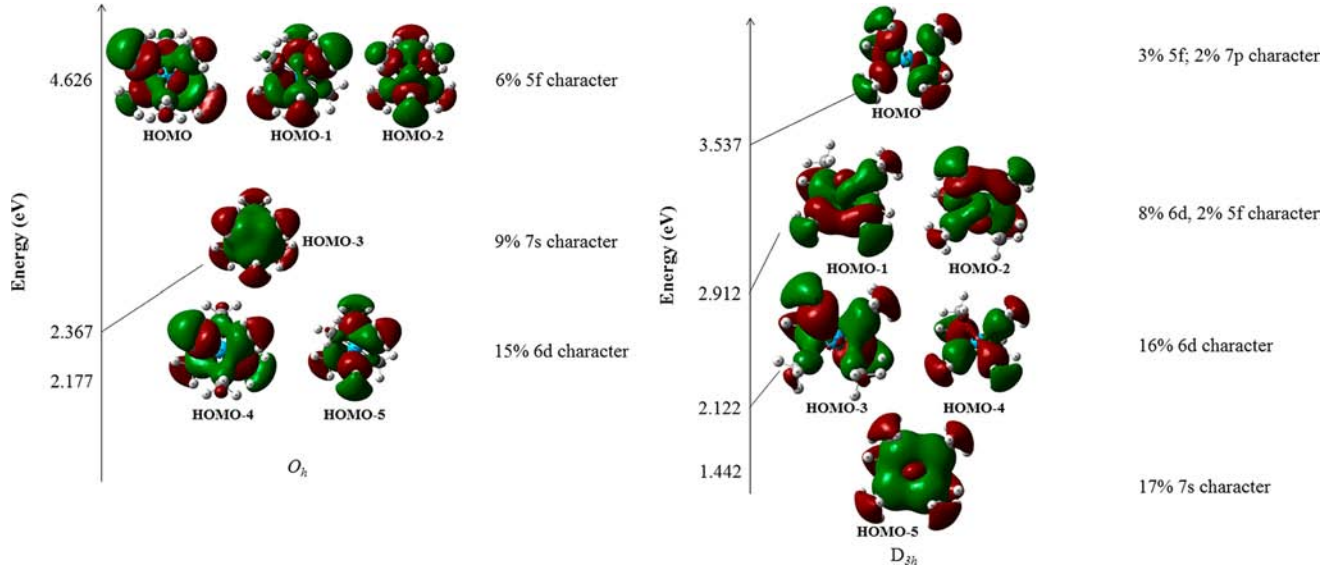

Figure 3. Bonding molecular orbitals of $[ThMe_6]^{2-}$ in O_h symmetry (left). Bonding molecular orbitals of $[ThMe_6]^{2-}$ in D_{3h} symmetry (right). Isolevel shown at 0.0250.

dx.doi.org/10.1021/ic300867m | Inorg. Chem. 2013, 52, 3556−3564

HOMO−3 and HOMO−4 (E″) are also doubly degenerate and contain 16% 6d character, while HOMO−5 (A'_1) contains 17% 7s character.

Clearly, the Th−C bonding interactions in D_{3h} $[ThMe_6]^{2-}$ are predicted to be quite ionic. For example, the largest thorium character is only 17% (HOMO−5), while three bonding molecular orbitals have less than 10% thorium character (HOMO, HOMO−1, and HOMO−2). This is also true in octahedral symmetry (Figure 3), where HOMO, HOMO−1, and HOMO−2 are triply degenerate and contain only 6% thorium (5f) character. HOMO−3 exhibits 9% 7s character, while doubly generate HOMO−4 and HOMO−5 have 15% 6d character.

As expected, the major difference between the O_h and D_{3h} geometries is participation of the 6d orbitals (Tables 1 and 2),

Table 1. Mulliken Populations and Orbital Energies for $[ThMe_6]^{2-}$ in D_{3h} Symmetry

orbital	energy (eV)	s	p	d	f	total	type
HOMO	3.537	0.00	0.02	0.00	0.03	0.05	$f_\sigma + p_\sigma$
HOMO−1	2.912	0.00	0.00	0.08	0.02	0.10	$d_\sigma + f_\sigma$
HOMO−2	2.912	0.00	0.00	0.08	0.02	0.10	$d_\sigma + f_\sigma$
HOMO−3	2.122	0.00	0.00	0.16	0.00	0.16	d_σ
HOMO−4	2.122	0.00	0.00	0.16	0.00	0.16	d_σ
HOMO−5	1.442	0.17	0.00	0.00	0.00	0.17	s_σ

Table 2. Mulliken Populations and Orbital Energies for $[ThMe_6]^{2-}$ in O_h Symmetry

orbital	energy (eV)	s	p	d	f	total	type
HOMO	4.626	0.00	0.00	0.00	0.06	0.06	f_σ
HOMO−1	4.626	0.00	0.00	0.00	0.06	0.06	f_σ
HOMO−2	4.626	0.00	0.00	0.00	0.06	0.06	f_σ
HOMO−3	2.367	0.09	0.00	0.00	0.00	0.09	s_σ
HOMO−4	2.177	0.00	0.00	0.15	0.00	0.15	d_σ
HOMO−5	2.177	0.00	0.00	0.15	0.00	0.15	d_σ

which are much more prominent in D_{3h} symmetry than in O_h symmetry. In D_{3h} symmetry, the 6d orbitals participate in HOMO−1, HOMO−2, HOMO−3, and HOMO−4, whereas they only participate in two Th−C molecular orbitals in O_h symmetry. This suggests a similar role for the 6d orbitals in the deviation of $[ThMe_6]^{2-}$ from octahedral, as is found for comparable transition-metal $[MR_6]^n$ complexes.[29,30] These results also complement the findings of Straka and Kaupp for $[AnH_6]^{2-}$ (An = Th, U),[65,66] who predicted that $[ThH_6]^{2-}$ should adopt a D_{3h} geometry with only a small amount f-orbital participation and much larger d-orbital participation.[65,66] Additionally, in $[ThMe_6]^{2-}$, the 7s contribution increases noticeably in going from O_h to D_{3h} symmetry. This occurs with a concomitant 0.925 eV lowering of the energy of this molecular orbital. This latter effect is somewhat unanticipated because a change in 7s orbital participation was not seen in previous calculations on $[ThH_6]^{2-}$ or $[ThF_6]^{2-}$.[65,66]

Calculations on complexes **1** and **3** were also conducted at the B3LYP level of theory. For **1**, HOMO through HOMO−4 correspond to the molecular orbitals involved in the Th−C bonds. The optimized geometry of **1** reveals a distorted trigonal-bipyramidal structure with approximate D_{3h} symmetry. The three C−Th−C bond angles for the equatorial $(CH_2CMe_3)^-$ groups were found to be 129.0, 118.5, and 112.5°. These values compare well with those observed in the crystal structure, namely, 132(1), 116.4(4), and 111.4(8)°. As was observed for $[ThMe_6]^{2-}$, the Th−C interactions are highly polarized and contain significant carbon 2p character with varying contributions of hybrid metal-based orbitals (Table 3).

Table 3. Mulliken Populations and Orbital Energies for $[Th(CH_2{}^tBu)_5]^-$ (1)

orbital	energy (eV)	s	p	d	f	total	type
HOMO	−1.333	0.02	0.00	0.07	0.07	0.16	$d_\sigma + f_\sigma + s_\sigma$
HOMO−1	−1.769	0.00	0.00	0.14	0.02	0.16	$d_\sigma + f_\sigma$
HOMO−2	−2.150	0.00	0.00	0.17	0.00	0.17	d_σ
HOMO−3	−2.503	0.06	0.00	0.12	0.00	0.18	$d_\sigma + s_\sigma$
HOMO−4	−2.803	0.11	0.00	0.08	0.03	0.22	$s_\sigma + d_\sigma + f_\sigma$

For example, HOMO contains both 7% 5f and 7% 6d character, while HOMO−1 (14% 6d), HOMO−2 (17% 6d), and HOMO−3 (12% 6d) show predominately 6d orbital participation. Additionally, HOMO−3 and HOMO−4 exhibit 6% and 11% 7s character, respectively. We have previously reported calculations on $[U(CH_2SiMe_3)_5]^-$ that reveal similar trends in the M−C bonding interactions.[20] However, the f-orbital participation is much greater in the uranium complex. For example, in $[U(CH_2SiMe_3)_5]^-$, HOMO−3 has 19% f character, whereas the maximum 5f character seen in any molecular orbital of **1** is 7%. This is consistent with the anticipated decrease in the f orbital energy on moving from thorium to uranium.[57]

A distorted octahedral geometry is predicted for complex **3**, which matches the observed geometry about the thorium center in the experimental structure. In particular, the equatorial benzyl groups display C−Th−C bond angles of 98.8, 78.6, 83.3, and 105.4°. The DFT calculations did not predict the presence of a multidentate benzyl ligand in **3**. Additionally, the potassium counterions were not used in the optimization. Complex **3** shows a similar pattern of small 5f and moderate 6d and 7s contributions, in which HOMO through HOMO−5 contain the Th−C bonding orbitals (Table 4).

Table 4. Mulliken Populations and Orbital Energies for $[Th(CH_2Ph)_6]^{2-}$ (3)

orbital	energy (eV)	s	p	d	f	total	type
HOMO	1.089	0.00	0.00	0.00	0.05	0.05	f_σ
HOMO−1	0.952	0.00	0.00	0.02	0.05	0.07	$f_\sigma + d_\sigma$
HOMO−2	0.843	0.00	0.00	0.06	0.04	0.10	$d_\sigma + f_\sigma$
HOMO−3	0.163	0.00	0.00	0.14	0.00	0.14	d_σ
HOMO−4	0.136	0.00	0.00	0.13	0.00	0.13	d_σ
HOMO−5	0.054	0.10	0.00	0.00	0.00	0.10	s_σ

Most importantly, the calculations reveal that the Th−C interactions in **3** are even more ionic than those in **1**. For example, HOMO, HOMO−1, and HOMO−2 (which comprise the t_{1u} set) only exhibit 5%, 7%, and 10% thorium character, respectively. Furthermore, as observed in **1**, complex **3** exhibits very little 5f character, and because of the O_h symmetry, only two orbitals have notable 6d character (i.e., HOMO−3 and HOMO−4, which exhibit 13% and 14% d character, respectively). In principle, complex **3** could increase d-orbtial participation by adopting a lower-symmetry geometry;

dx.doi.org/10.1021/ic300867m | Inorg. Chem. 2013, 52, 3556−3564

however, we suspect that **3** remains octahedral as a result of steric considerations because the benzyl groups may not be able to accommodate the smaller C−Th−C angles required for D_{3h} symmetry.

CONCLUDING REMARKS

The reaction of $ThCl_4(DME)_2$ with several common alkylating reagents provides a series of homoleptic thorium alkyl complexes, namely, $[Li(THF)_4][Th(CH_2{}^tBu)_5]$, $[Li(DME)_2][Th(CH_2SiMe_3)_5]$, and $[K(THF)]_2[Th(CH_2Ph)_6]$. These complexes were pursued in an effort to determine their geometries and thereby gain insight into d-orbital participation in actinide−ligand bonding. As with their closely related uranium analogues, these complexes are thermally sensitive in solution, decomposing rapidly in a variety of solvents. $[Th(CH_2{}^tBu)_5]^-$ exhibits a trigonal-bipyramidal geometry in the solid state, while the benzyl complex $[Th(CH_2Ph)_6]^{2-}$ exhibits an octahedral geometry in the solid state. DFT calculations on these materials reveal highly ionic Th−C interactions with very little 5f character in the Th−C bonds but somewhat more 6d character. Several attempts to prepare $[ThMe_6]^{2-}$ were unsuccessful. Interestingly, however, this material is predicted by DFT to exhibit D_{3h} symmetry, similar to the previously studied transition-metal hexa(methyl) complexes. Ultimately, the challenge of demonstrating d-orbital participation in An−L bonding by observation of a non-octahedral (D_{3h} or C_{3v}) geometry has yet to be achieved. Future success in this area will likely require the use of alkyl ligands with different steric and electronic properties than those used in this study.

EXPERIMENTAL SECTION

General Procedures. All reactions and subsequent manipulations were performed under anaerobic and anhydrous conditions under an atmosphere of argon or nitrogen. Diethyl ether, hexanes, and tetrahydrofuran (THF) were dried using a Vacuum Atmospheres DRI-SOLV solvent purification system. Dimethoxyethane (DME) was distilled from sodium benzophenone ketyl. All deuterated solvents were purchased from Cambridge Isotope Laboratories Inc. and were dried over activated 4 Å sieves for 24 h prior to use. $ThCl_4(DME)_2$, $[Li(TMEDA)]_3[ThMe_7]$, $LiCH_2{}^tBu$, and $K(CH_2Ph)$ were prepared according to published procedures.[23,87−89] All other reagents were obtained from commercial sources and used as received.

NMR spectra were recorded on a Varian UNITY INOVA 400 MHz spectrometer, a Varian UNITY INOVA 500 MHz spectrometer, or a Varian UNITY INOVA AS600 600 MHz spectrometer. ^1H and $^{13}C\{^1H\}$ NMR spectra are referenced to external $SiMe_4$ using the residual protio solvent peaks as internal standards (^1H NMR experiments) or the characteristic resonances of the solvent nuclei (^{13}C NMR experiments). $^7Li\{^1H\}$ NMR spectra are referenced to an external saturated solution of LiCl in deuterium oxide. Elemental analyses were performed by the Micro-Mass Facility at the University of California, Berkeley.

Computational Details. The electronic structures of $[Th(CH_2Ph)_6]^{2-}$, $[Th(CH_2{}^tBu)_5]^-$, and $[ThMe_6]^{2-}$ were examined using the *Gaussian09* software program[90] at the B3LYP level.[91,92] Full geometry optimizations were performed and stationary points were determined to be global minima using analytical frequency calculations with the Stuttgart/Dresden triple-ζ quality basis set[93] and the corresponding effective core potential for thorium. The most diffuse s, p, d, and f functions were removed, leaving 7s/6p/5d/3f. The Pople double-ζ quality basis set, 6-31G(d′),[94] was used for the carbon and hydrogen atoms. Mulliken population analyses on all compounds were performed to determine orbital involvement.

$[Li(THF)_4][Th(CH_2{}^tBu)_5]$ (1). To a cold (−25 °C), stirring solution of $ThCl_4(DME)_2$ (135 mg, 0.24 mmol) in THF (2 mL) was added a cold solution of $LiCH_2{}^tBu$ (95 mg, 1.21 mmol) in Et_2O (3 mL). This resulted in the immediate generation of a pale-yellow solution concomitant with the formation of a white precipitate. The solution was allowed to stir for 10 min, whereupon the volatiles were removed in vacuo and the resulting oil was extracted into Et_2O (4 mL). The solution was filtered through a Celite column (2 cm × 0.5 cm) supported on glass wool, and the volume of the filtrate was reduced in vacuo. The solution was layered with hexanes (2 mL), and subsequent storage at −25 °C for 24 h resulted in the deposition of colorless crystals (108 mg, 50% yield). ^1H NMR (500 MHz, 25 °C, THF-d_8): δ 3.54 (s, 16H, α-THF), 1.70 (s, 16H, β-THF), 1.02 (s, 45H, CH_3), −0.07 (s, 10H, CH_2). $^7Li\{^1H\}$ NMR (194 MHz, 25 °C, THF-d_8): δ 0.50 (s). $^{13}C\{^1H\}$ NMR (125 MHz, 25 °C, THF-d_8): δ 117.96 (s, CH_2 methylene), 39.14 (s, C *tert*-butyl), 37.58 (s, CH_3 *tert*-butyl). Anal. Calcd for $C_{41}H_{87}LiO_4Th$: C, 55.76; H, 9.93. Found: C, 55.60; H, 10.18.

$[Li(DME)_2][Th(CH_2SiMe_3)_5]$ (2). A cold (−25 °C) solution of $ThCl_4(DME)_2$ (153 mg, 0.28 mmol) in THF (2 mL) was added to a cold (−25 °C) stirring solution of $LiCH_2SiMe_3$ (130 mg, 1.38 mmol) in Et_2O (3 mL). This resulted in the immediate generation of a pale-yellow solution concomitant with the formation of a white precipitate. The solution was allowed to stir for 15 min, whereupon the white precipitate was removed by filtration through a Celite column (2 cm × 0.5 cm) supported on glass wool. The volatiles were removed in vacuo, and the resulting oil was extracted into Et_2O (4 mL). The solution was again filtered through a Celite column (2 cm × 0.5 cm) supported on glass wool. DME (0.5 mL) was subsequently added to the filtrate. The solution was layered with hexanes (3 mL), and subsequent storage at −25 °C for 24 h resulted in the deposition of colorless oil. The oil was rinsed with hexanes (3 × 1 mL) and subsequently dried in vacuo to give a white microcrystalline powder (127 mg, 54% yield). ^1H NMR (400 MHz, 25 °C, THF-d_8): δ 3.43 (s, 8H, CH_2 DME), 3.27 (s, 12H, CH_3 DME), −0.01 (s, 45H, CH_3), −0.63 (s, 10H, CH_2). $^7Li\{^1H\}$ NMR (155 MHz, 25 °C, THF-d_8): δ −0.53 (s). $^{13}C\{^1H\}$ NMR (151 MHz, 25 °C, THF-d_8): δ 82.97 (s, CH_2), 72.93 (s, CH_2 DME), 59.07 (s, CH_3 DME), 5.08 (s, CH_3). Anal. Calcd for $C_{28}H_{75}LiO_4Si_5Th$: C, 39.32; H, 8.84. Found: C, 39.26; H, 8.67.

$[K(THF)]_2[Th(CH_2Ph)_6]$ (3). To a cold (−25 °C), stirring solution of $ThCl_4(DME)_2$ (217 mg, 0.391 mmol) in THF (2 mL) was added a cold solution of $K(CH_2Ph)$ (305 mg, 2.34 mmol) in THF (3 mL). This resulted in the formation of a red-orange solution and a gray precipitate. The solution was allowed to stir for 10 min, whereupon the solution was filtered through a Celite column (2 cm × 0.5 cm) supported on glass wool and the volume of the filtrate was reduced in vacuo. The solution was layered with hexanes (2 mL), and storage of this solution at −25 °C for 24 h resulted in the deposition of a yellow-orange powder (312 mg, 80% yield). X-ray-quality crystals were grown from a dilute THF solution layered with Et_2O. ^1H NMR (500 MHz, 25 °C, THF-d_8): δ 6.69 (s, 12H, *o*-CH), 6.27 (s, 12H, *m*-CH), 6.11 (s, 6H, *p*-CH), 3.54 (s, 8H, α-THF), 1.69 (s, 8H, β-THF), 1.34 (s, 12H, CH_2). $^{13}C\{^1H\}$ NMR (125 MHz, 0 °C, THF-d_8): δ 153.0 (br s, *ipso*-C), 124.1 (br s, *m*-CH, *o*-CH), 115.9 (br s, *p*-CH), 89.6 (br s, CH_2). Anal. Calcd for $C_{50}H_{58}K_2O_2Th$: C, 59.98; H, 5.84. Found: C, 57.61; H, 5.31. The carbon percentage was found to be low over several measurements, likely because of the thermal instability of the material.

X-ray Crystallography. Data for **3** were collected on a Bruker 3-axis platform diffractometer equipped with a SMART-1000 CCD detector using a graphite monochromator with a Mo Kα X-ray source (α = 0.71073 Å). A hemisphere of data was collected at 150(2) K using ω scans with 0.3° frame widths, using 25 s frame exposures. Data for **1** were collected on a Bruker Proteum2 diffractometer equipped with a PLATINUM CCD detector using multilayer optics with a Cu Kα X-ray source (α = 1.4178 Å). The crystals of **1** were mounted on a cryoloop under Paratone-N oil, and all data were collected at 100(2) K using an Oxford nitrogen gas cryostream system. Frame exposures of 7 s were used for **1**. Data collection and cell parameter determination were conducted using the *SMART* program.[95] Integration of the data frames and final cell parameter refinement were performed using *SAINT* software.[96] Absorption correction of the data for **1** was carried out using the multiscan method *SADABS*,[97] while the absorption

dx.doi.org/10.1021/ic300867m | *Inorg. Chem.* 2013, 52, 3556−3564

correction of the data for **3** was carried out empirically based on reflection ψ scans. Subsequent calculations were carried out using *SHELXTL*.[98] Structure determination was done using direct or Patterson methods and difference Fourier techniques. All hydrogen-atom positions were idealized and rode on the atom of attachment, with exceptions noted in the subsequent paragraph. Structure solution, refinement, graphics, and creation of publication materials were performed using *SHELXTL*.[98] A summary of relevant crystallographic data is presented in Table 5.

Table 5. X-ray Crystallographic Data for Complexes 1 and 3

	1	3
empirical formula	$C_{41}H_{87}LiO_4U$	$C_{50}H_{58}K_2O_2U$
cryst habit, color	rod, colorless	block, orange
cryst size (mm)	0.30 × 0.20 × 0.05	0.70 × 0.50 × 0.15
cryst syst	orthorhombic	monoclinic
space group	$P2_12_12_1$	Pn
volume (Å^3)	9459.9(6)	4607(2)
a (Å)	10.3960(4)	9.341(3)
b (Å)	16.7648(7)	29.955(7)
c (Å)	54.2778(18)	16.497(4)
α (deg)	90	90
β (deg)	90	93.604(10)
γ (deg)	90	90
Z	8	4
fw (g/mol)	883.09	1001.20
density (calcd) (Mg/m^3)	1.240	1.444
abs coeff (mm^{-1})	10.399	3.454
F_{000}	3664	2008
total no. of reflns	31125	37828
unique reflns	13407	17026
final R indices [$I > 2\sigma(I)$]	R1 = 0.0830, wR2 = 0.2306	R1 = 0.0536, wR2 = 0.1075
largest diff peak and hole (e/Å^3)	2.467 and −1.937	3.475 and −1.656
GOF	1.162	0.992

For complex **1**, several carbon atoms were refined isotropically due to disorder. For complex **3**, a THF molecule was disordered over two positions in a 50:50 ratio. Hydrogen atoms were not assigned to disordered carbon atoms.

■ ASSOCIATED CONTENT

Supporting Information

Experimental procedures, crystallographic details (as CIF files), and spectral data for **1**−**3**, optimized Cartesian coordinates for $[ThMe_6]^{2-}$, **1**, and **3**, and the complete version of ref 90. This material is available free of charge via the Internet at http://pubs.acs.org.

■ AUTHOR INFORMATION

Corresponding Author

*E-mail: hayton@chem.ucsb.edu (T.W.H.), walenskyj@missouri.edu (J.R.W.).

Notes

The authors declare no competing financial interest.

■ ACKNOWLEDGMENTS

Research at the University of California, Santa Barbara, was supported by the U.S. Department of Energy, Office of Basic Energy Sciences, Chemical Sciences, Biosciences, and Geosciences Division under Contract DE-FG02-09ER16067. J.R.W. gratefully acknowledges the U.S. Department of Homeland Security's National Technical Nuclear Forensics Center and U.S. Nuclear Regulatory Commission for support.

■ REFERENCES

(1) Gilman, H.; Jones, R. G.; Bindschadler, E.; Blume, D.; Karmas, G.; Martin, G. A.; Nobis, J. F.; Thirtle, J. R.; Yale, H. L.; Yoeman, F. A. *J. Am. Chem. Soc.* **1956**, *78*, 2790−2792.
(2) Gilman, H. *Adv. Organomet. Chem.* **1968**, *7*, 33.
(3) Marks, T. J.; Seyam, A. M. *J. Organomet. Chem.* **1974**, *67*, 61−66.
(4) Sigurdson, E. R.; Wilkinson, G. *Dalton Trans.* **1977**, 812−818.
(5) Cernia, E.; Mazzei, A. *Inorg. Chim. Acta* **1974**, *10*, 239−252.
(6) Evans, W. J.; Wink, D. J.; Stanley, D. R. *Inorg. Chem.* **1982**, *21*, 2565−2573.
(7) Seyam, A. M. *Inorg. Chim. Acta* **1983**, *77*, L123−125.
(8) Van der Sluys, W. G.; Burns, C. J.; Sattelberger, A. P. *Organometallics* **1989**, *8*, 855−857.
(9) Marks, T. J. *J. Organomet. Chem.* **1975**, *95*, 301−315.
(10) Streitweiser, A. Preparation and Chemistry of Uranocenes. In *Organometallics of the f-Elements*; Marks, T. J., Fischer, R. D., Eds.; D. Reidel Publishing: Dordrecht, Holland, 1978; p 154.
(11) Miller, M. J.; Streitwieser, A. *J. Organomet. Chem.* **1981**, *209*, C52−C54.
(12) Marks, T. J. *Prog. Inorg. Chem.* **1979**, *25*, 223−333.
(13) Thiele, K. H.; Opitz, R.; Köhler, E. *Z. Anorg. Allg. Chem.* **1977**, *435*, 45−48.
(14) Edwards, P. G.; Andersen, R. A.; Zalkin, A. *Organometallics* **1984**, *3*, 293−398.
(15) Edwards, P. G.; Andersen, R. A.; Zalkin, A. *J. Am. Chem. Soc.* **1981**, *103*, 7792−7794.
(16) Stewart, J. L.; Andersen, R. A. *Polyhedron* **1998**, *17*, 953−958.
(17) Ortiz, J. V.; Hay, P. J.; Martin, R. L. *J. Am. Chem. Soc.* **1992**, *114*, 2736−2737.
(18) Hay, P. J.; Martin, R. L. *J. Alloys Compd.* **1994**, *213*, 196−198.
(19) Fortier, S.; Melot, B. C.; Wu, G.; Hayton, T. W. *J. Am. Chem. Soc.* **2009**, *131*, 15512−15521.
(20) Fortier, S.; Walensky, J. R.; Wu, G.; Hayton, T. W. *J. Am. Chem. Soc.* **2011**, *133*, 11732−11743.
(21) Kraft, S. J.; Fanwick, P. E.; Bart, S. C. *J. Am. Chem. Soc.* **2012**, *134*, 6160−6168.
(22) Duhovic, S.; Khan, S.; Diaconescu, P. L. *Chem. Commun.* **2010**, *46*, 3390−3392.
(23) Lauke, H.; Swepston, P. J.; Marks, T. J. *J. Am. Chem. Soc.* **1984**, *106*, 6841−6843.
(24) Shannon, R. D. *Acta Crystallogr.* **1976**, *A32*, 751−767.
(25) Eisen, M. S.; Marks, T. J. *J. Am. Chem. Soc.* **1992**, *114*, 10358−10368.
(26) Kohler, E.; Bruser, W.; Thiele, K.-H. *J. Organomet. Chem.* **1974**, *76*, 235−240.
(27) Cruz, C. A.; Emslie, D. J. H.; Harrington, L. E.; Britten, J. F.; Robertson, C. M. *Organometallics* **2007**, *26*, 692−701.
(28) Demolliens, A.; Jean, Y.; Eisenstein, O. *Organometallics* **1986**, *5*, 1457−1464.
(29) Kang, S. K.; Albright, T. A.; Eisenstein, O. *Inorg. Chem.* **1989**, *28*, 1611−1613.
(30) Kang, S. K.; Tang, H.; Albright, T. A. *J. Am. Chem. Soc.* **1993**, *115*, 1971−1981.
(31) Tanpipat, N.; Baker, J. *J. Phys. Chem.* **1996**, *100*, 19818−19823.
(32) Kaupp, M. *J. Am. Chem. Soc.* **1996**, *118*, 3018−3024.
(33) Kaupp, M. *Chem.—Eur. J.* **1998**, *4*, 1678−1686.
(34) Kaupp, M. *Angew. Chem., Int. Ed.* **2001**, *40*, 3534−3575.
(35) Pfennig, V.; Seppelt, K. *Science* **1996**, *271*, 626−628.
(36) Kleinhenz, S.; Pfennig, V.; Seppelt, K. *Chem.—Eur. J.* **1998**, *4*, 1687−1691.
(37) Seppelt, K. *Acc. Chem. Res.* **2003**, *36*, 147−153.
(38) Morse, P. M.; Girolami, G. S. *J. Am. Chem. Soc.* **1989**, *111*, 4114−4116.
(39) Landis, C. R.; Cleveland, T.; Firman, T. K. *J. Am. Chem. Soc.* **1995**, *117*, 1859−1860.

(40) Landis, C. R.; Firman, T. K.; Root, D. M.; Cleveland, T. *J. Am. Chem. Soc.* **1998**, *120*, 1842−1852.
(41) Landis, C. R.; Cleveland, T.; Firman, T. K. *J. Am. Chem. Soc.* **1998**, *120*, 2641−2649.
(42) Jonas, V.; Frenking, G.; Gauss, J. *Chem. Phys. Lett.* **1992**, *194*, 109−117.
(43) Shortland, A. J.; Wilkinson, G. *J. Chem. Soc., Dalton Trans.* **1973**, 872−876.
(44) Galyer, A. L.; Wilkinson, G. *J. Chem. Soc., Dalton Trans.* **1976**, 2235−2238.
(45) Haaland, A.; Hammel, A.; Rypdal, K.; Volden, H. V. *J. Am. Chem. Soc.* **1990**, *112*, 4547−4549.
(46) Vaid, T. P.; Veige, A. S.; Lobkovsky, E. B.; Glassey, W. V.; Wolczanski, P. T.; Liable-Sands, L. M.; Rheingold, A. L.; Cundari, T. R. *J. Am. Chem. Soc.* **1998**, *120*, 10067−10079.
(47) El-Kurdi, S.; Seppelt, K. *Chem.—Eur. J.* **2011**, *17*, 3956−3962.
(48) Kleinhenz, S.; Schubert, M.; Seppelt, K. *Chem. Ber.* **1997**, *130*, 903−906.
(49) Friese, J. C.; Krol, A.; Puke, C.; Kirschbaum, K.; Giolando, D. M. *Inorg. Chem.* **2000**, *39*, 1496−1500.
(50) Hoffmann, R.; Howell, J. M.; Rossi, A. R. *J. Am. Chem. Soc.* **1976**, *98*, 2484−2492.
(51) McGrady, G. S.; Downs, A. J. *Coord. Chem. Rev.* **2000**, *197*, 95−124.
(52) Cremades, E.; Echeverría, J.; Alvarez, S. *Chem.—Eur. J.* **2010**, *16*, 10380−10396.
(53) Denning, R. *Struct. Bonding (Berlin)* **1992**, *79*, 215−276.
(54) Denning, R. G. *J. Phys. Chem. A* **2007**, *111*, 4125−4143.
(55) Denning, R. G.; Green, J. C.; Hutchings, T. E.; Dallera, C.; Tagliaferri, A.; Giarda, K.; Brookes, N. B.; Braicovich, L. *J. Chem. Phys.* **2002**, *117*, 8008−8020.
(56) Prodan, I. D.; Scuseria, G. E.; Martin, R. L. *Phys. Rev. B* **2007**, *76*, 033101.
(57) Walensky, J. R.; Martin, R. L.; Ziller, J. W.; Evans, W. J. *Inorg. Chem.* **2010**, *49*, 10007−10012.
(58) Kozimor, S. A.; Yang, P.; Batista, E. R.; Boland, K. S.; Burns, C. J.; Clark, D. L.; Conradson, S. D.; Martin, R. L.; Wilkerson, M. P.; Wolfsberg, L. E. *J. Am. Chem. Soc.* **2009**, *131*, 12125−12136.
(59) Arnold, P.; Turner, Z.; Kaltsoyannis, N.; Pelekanaki, P.; Bellabarba, R.; Tooze, R. *Chem.—Eur. J.* **2010**, *16*, 9623−9629.
(60) Raymond, K. N.; Eigenbrot, C. W. *Acc. Chem. Res.* **1980**, *13*, 276−283.
(61) Cantat, T.; Graves, C. R.; Jantunen, K. C.; Burns, C. J.; Scott, B. L.; Schelter, E. J.; Morris, D. E.; Hay, P. J.; Kiplinger, J. L. *J. Am. Chem. Soc.* **2008**, *130*, 17537−17551.
(62) Li, J.; Bursten, B. E. *J. Am. Chem. Soc.* **1997**, *119*, 9021−9032.
(63) Tassell, M. J.; Kaltsoyannis, N. *Dalton Trans.* **2010**, *39*, 6719−6725.
(64) Ingram, K. I. M.; Kaltsoyannis, N.; Gaunt, A. J.; Neu, M. P. *J. Alloys Compd.* **2007**, *444−445*, 369−375.
(65) Straka, M.; Hrobarik, P.; Kaupp, M. *J. Am. Chem. Soc.* **2005**, *127*, 2591−2599.
(66) Straka, M.; Patzschke, M.; Pyykko, P. *Theor. Chem. Acc.* **2003**, *109*, 332−340.
(67) Minasian, S. G.; Keith, J. M.; Batista, E. R.; Boland, K. S.; Clark, D. L.; Conradson, S. D.; Kozimor, S. A.; Martin, R. L.; Schwarz, D. E.; Shuh, D. K.; Wagner, G. L.; Wilkerson, M. P.; Wolfsberg, L. E.; Yang, P. *J. Am. Chem. Soc.* **2012**, *134*, 5586−5597.
(68) King, R. B. *Inorg. Chem.* **1992**, *31*, 1978−1980.
(69) King, R. B. *Inorg. Chem.* **1998**, *37*, 3057−3059.
(70) Cameron, A. D.; Fitzgerald, G.; Zerner, M. C. *Inorg. Chem.* **1988**, *27*, 3437−3439.
(71) Schumann, H.; Mueller, J.; Bruncks, N.; Lauke, H.; Pickardt, J.; Schwarz, H.; Eckart, K. *Organometallics* **1984**, *3*, 69−74.
(72) Schumann, H.; Pickardt, J.; Bruncks, N. *Angew. Chem., Int. Ed.* **1981**, *20*, 120−121.
(73) Schumann, H.; Lauke, H.; Hahn, E.; Pickardt, J. *J. Organomet. Chem.* **1984**, *263*, 29−35.
(74) Bursten, B. E.; Strittmatter, R. J. *Angew. Chem., Int. Ed.* **1991**, *30*, 1069−1085.
(75) Bruno, J. W.; Smith, G. M.; Marks, T. J.; Fair, C. K.; Schultz, A. J.; Williams, J. M. *J. Am. Chem. Soc.* **1986**, *108*, 40−56.
(76) Butcher, R. J.; Clark, D. L.; Grumbine, S. K.; Scott, B. L.; Watkin, J. G. *Organometallics* **1996**, *15*, 1488−1496.
(77) Fredrick, C. M.; Mintz, E. A.; Schertz, L. D.; Marks, T. J.; Day, V. W. *Organometallics* **1984**, *3*, 819−821.
(78) Scholz, J.; Rehbaum, F.; Thiele, K.-H.; Goddard, R.; Betz, P.; Kruger, C. *J. Organomet. Chem.* **1993**, *443*, 93−99.
(79) Bassi, I. W.; Allegra, G.; Scordamaglia, R.; Chioccola, G. *J. Am. Chem. Soc.* **1971**, *93*, 3787−3788.
(80) Monreal, M. J.; Diaconescu, P. L. *Organometallics* **2008**, *27*, 1702−1706.
(81) Kiplinger, J. L.; Morris, D. E.; Scott, B. L.; Burns, C. J. *Organometallics* **2002**, *21*, 5978−5982.
(82) Jantunen, K. C.; Burns, C. J.; Castro-Rodriguez, I.; Da Re, R. E.; Golden, J. T.; Morris, D. E.; Scott, B. L.; Taw, F. L.; Kiplinger, J. L. *Organometallics* **2004**, *23*, 4682−4692.
(83) Perego, G.; Cesari, M.; Farina, F.; Lugli, G. *Acta Crystallogr., Sect. B* **1976**, *32*, 3034.
(84) Meyer, N.; Roesky, P. W.; Bambirra, S.; Meetsma, A.; Hessen, B.; Saliu, K.; Takats, J. *Organometallics* **2008**, *27*, 1501−1505.
(85) Chitsaz, S.; Neumuller, B. *Organometallics* **2001**, *20*, 2338−2343.
(86) Andrews, P.; Kennedy, A. R.; Mulvey, R. E.; Raston, C. L.; Roberts, B. A.; Rowlings, R. B. *Angew. Chem., Int. Ed.* **2000**, *39*, 1960−1962.
(87) Cantat, T.; Scott, B. L.; Kiplinger, J. L. *Chem. Commun.* **2010**, *46*, 919−921.
(88) Schlosser, M.; Hartmann, J. *Angew. Chem., Int. Ed.* **1973**, *12*, 508−509.
(89) Schrock, R. R.; Fellmann, J. D. *J. Am. Chem. Soc.* **1978**, *100*, 3359−3370.
(90) Frisch, M. J.; et al. *Gaussian 09*, revision A.02; Gaussian, Inc.: Wallington, CT, 2009.
(91) Becke, A. D. *J. Chem. Phys.* **1993**, *98*, 5648−5652.
(92) Stephens, P. J.; Devlin, F. J.; Chabalowski, C. F.; Frisch, M. J. *J. Phys. Chem.* **1994**, *98*, 11623−11627.
(93) Kuechle, W.; Dolg, M.; Stoll, H.; Preuss, H. *J. Chem. Phys.* **1994**, *100*, 7535−7542.
(94) Petersson, G. A.; Bennett, A.; Tensfeldt, T. G.; Al-Laham, M. A.; Shirley, W. A.; Mantzaris, J. *J. Chem. Phys.* **1988**, *89*, 2193−2218.
(95) *SMART Software Users Guide*, version 5.1; Bruker Analytical X-ray Systems, Inc.: Madison, WI, 1999.
(96) *SAINT Software User's Guide*, version 5.1; Bruker Analytical X-ray Systems, Inc.: Madison, WI, 1999.
(97) Sheldrick, G. M. *SADABS*; University of Gottingen: Gottingen, Germany, 2005.
(98) Sheldrick, G. M. *SHELXTL*, version 6.12; Bruker Analytical X-ray Systems, Inc.: Madison, WI, 2001.